European Journal of Pharmaceutical Sciences 202 (2024) 106892

Contents lists available at ScienceDirect

European Journal of Pharmaceutical Sciences

journal homepage: www.elsevier.com/locate/ejps

Novel analytical solutions for convolution in compartmental pharmacokinetic models and application to non-bioequivalent formulations

Mauricio A. García [a,*], Pablo M. González [b], Alexis Aceituno [c,d], Jozef Al-Gousous [e,f]

[a] Departamento de Farmacia, Escuela de Química y Farmacia, Facultad de Química y de Farmacia, Pontificia Universidad Católica de Chile, Santiago, 7820436, Chile
[b] Innovation and Biopharmaceutical Evaluation Center (IBECenter), Santiago, Chile
[c] National Drug Agency Department, Institute of Public Health (ISP), Santiago, Chile
[d] Facultad de Farmacia, Universidad de Valparaíso, Valparaíso, Chile
[e] Departament of Biopharmaceutics and Pharmaceutical Technology, Johannes Gutenberg University Mainz, 55099, Mainz, Germany
[f] Departament of Pharmaceutical Sciences, University of Michigan, 428 Church Street, Ann Arbor, MI, 48109, USA

ARTICLE INFO

Keywords:
Convolution
Deconvolution
Analytical solution
Loo Riegelman
Correlation
Bioinequivalence
Levonorgestrel

ABSTRACT

Deconvolution and convolution are powerful tools that allow decomposition and reconstruction, respectively, of plasma versus time profiles from input and impulse functions. While deconvolution have commonly used compartmental approaches (e.g., Wagner-Nelson or Loo-Riegelman), convolution most typically used the convolution integral which can be solved with numerical methods. In 2005, an analytical solution for one-compartment pharmacokinetic was proposed and has been widely used ever since. However, to the best of our knowledge, analytical solutions for drugs distributed in more than one compartment have not been reported yet. In this paper, analytical solutions for compartmental convolution from both original and exact Loo-Riegelman approaches were developed and evaluated for different scenarios. While convolution from original approach was slightly more precise than that from the exact Loo-Riegelman, both methods were extremely accurate for reconstruction of plasma profiles after respective deconvolutions. Nonetheless, convolution from exact Loo-Riegelman was easier to interpret and to be manipulated mathematically. In fact, convolution solutions for three and more compartments can be easily written with this approach. Finally, our convolution analytical solution was applied to predict the failure in bioequivalence for levonorgestrel, demonstrating that equations in this paper may be useful tools for pharmaceutical scientists.

1. Introduction

Convolution and deconvolution are powerful tools for assessing drug product performance. While the latter allows the estimation of the fraction absorbed over time from plasma concentration time profiles, the former is the reconstruction of plasma levels from an input (fraction absorbed) and an impulse (distribution/elimination) function (both dependent on time). Application of these procedures is broad in pharmaceutical industry, including development of in vitro in vivo correlations (IVIVCs), guidance of rational drug development, assessment of biopredictivity for dissolution media, dissolution specification setting, application to scale-up post-approval changes (SUPAC), among many others (Davanço et al., 2020; Sjögren et al., 2014; U.S. Department of Health and Human Services Food and Drug Administration Center for Drug Evaluation and Research (CDER), 1997, 1995). With these tools, it is expected that the number of clinical trials is reduced, because new formulations may be tested in vitro, while predicting plasma concentrations via convolution (e.g., through an IVIVC). This has clear advantages not only on ethical concerns associated with unnecessary in vivo studies, but also because of expensive and time-consuming clinical trials. In this regard, deconvolution/convolution approaches can be used to link differences in in vitro product performance with a failure in their bioequivalence. This linkage may be key to find a biopredictive method to guide the rational drug development. Accordingly, convolution of in vitro dissolution profiles, at relevant time-scales, may be used as input function to predict drug product performance in vivo.

Abbreviations: AUC, Area under the curve; BE, Bioequivalence; ER, Extended-Release; F_a, Fraction absorbed; F_d, Fraction dissolved; IS, Ionic strength; IR, Immediate-Release; IV, Intravenous; IVIVC, In vitro in vivo correlation; PBBM, Physiologically-based biopharmaceutic model; PE, Prediction error; PK, Pharmacokinetics; RMSE, Root mean squared error; SUPAC, scale-up post-approval changes; Vc, Volume of central compartment.

* Corresponding author.
E-mail address: magarci3@uc.cl (M.A. García).

https://doi.org/10.1016/j.ejps.2024.106892
Received 18 May 2024; Received in revised form 3 August 2024; Accepted 3 September 2024
Available online 6 September 2024

After deconvolution, diverse strategies have been used for convoluting plasma concentration profiles. While some approaches include the superposition principle (Langenbucher, 2003; Qureshi, 2010), some others involve curve fitting methods (González-García et al., 2015) in numerical differential equation solver software. Furthermore, reconstruction of plasma profiles may be also achieved by convolution integral in a model-independent approach (Krishna and Yu, 2008). Even though this is the most popular method, it is mainly applied to direct convolution approaches which requires of a time-scaling function (Al-Gousous and Langguth, 2018; González-García et al., 2015; Krishna and Yu, 2008). Moreover, model-independent convolution integral can be only solved through numerical methods. By contrast, plasma profile deconvolution may typically use compartmental methods (Bermejo et al., 2020a) or, more recently, physiologically-based biopharmaceutic models (PBBM) (Madny et al., 2022). Either way, comprehensive analytical equations for solving compartmental convolution have only barely been explored.

In 2005, Gohel et al.,(Gohel et al., 2005) deduced a simple analytical solution for convoluting plasma profiles from fraction absorbed plots, by using the mass balance principle proposed by Wagner-Nelson in 1963 (Wagner and Nelson, 1963). This is advantageous not only because of the straightforward calculation method, but it also provides a comprehensive mathematical model to understand the relations between elimination and absorption rates, resulting in the plasma concentration time profile. That is why several studies have used that equation to back-calculate plasma profiles in diverse applications. (González-García et al., 2015; Salehi et al., 2021; Sánchez-Dengra et al., 2021; Taha and Emara, 2022; Yaro et al., 2014) In spite of these advantages, the application of Gohel's equation is specific to drugs with one-compartment pharmacokinetics (PK). Therefore, more general approaches are needed to cover majority of drugs, as they typically exhibit two-compartmental PK after extravascular administration (Liu et al., 2023), as well as those cases with three-compartmental PK. To the best of our knowledge, comprehensive equations for the aforementioned cases have not been reported so far.

The aim of this paper was to apply an analogue approach as the one published by Gohel et al.,(Gohel et al., 2005) to derive analytical solutions for two and even three compartment PK. Original deconvolution equation proposed by Loo-Riegelman for two compartment PK, (Loo and Riegelman, 1968), as well as its exact solution, reported by John Wagner,(Wagner, 1983) were used as starting points. Deduced equations were verified using cases representing relatively rapid distribution (ketoprofen), slow distribution (amlodipine) and different absorption rates (modified-release theophylline oral formulations). Finally, an analytical solution for compartmental convolution was successfully used to get insights in the failure of bioequivalence for levonorgestrel-containing immediate release (IR) tablets. The equation successfully predicted plasma levels from in vitro dissolution in biopredictive media. We foresee these analytical solutions will be highly appreciated by pharmaceutical scientists allowing not only a straightforward computation of compartmental convolution, but also enabling a comprehensive understanding of the convolution procedure.

2. Meterials and methods

2.1. Theory

2.1.1. Convolution equation from original Loo-Riegelman method

Assuming drug absorption is completed with negligible first pass extraction, and distribution/elimination follows a two compartment PK, the original Loo-Riegelman method (Loo and Riegelman, 1968) can be applied to deconvolute the fraction absorbed (F_a), as the ratio of the amount absorbed at time=t ($X_{a,t}$) to the total amount absorbed ($X_{a,\infty}$):

$$F_{a,t} = \frac{X_{a,t}}{X_{a,\infty}} = \frac{\left(C_{c,t} + C_{p,t} + \left(k_{10}\int_0^t C_c dt\right)\right)}{\left(k_{10}\int_0^\infty C_c dt\right)} \quad (1)$$

In this equation, C_c and C_p are drug concentrations in the central and peripheral compartments, respectively, k_{10} is the elimination micro-constant from central compartment, and t is the time. Applying the rationale proposed by Gohel et al., (Gohel et al., 2005) plasma concentrations at $t=t_{+1}$ ($C_{c,t+1}$) can be calculated as a function of the difference between of F_a ($\Delta F_a = F_{a,t+1} - F_{a,t}$) and time ($\Delta t = t_{+1} - t$) as per Eq. (2):

$$C_{c,t+1} = \frac{\Delta F_a\left(\frac{X_0}{V_c}\right) + \left(C_{c,t}\left(1 - \frac{k_{10}(\Delta t)}{2}\right)\right) - \left(C_{p,t+1} - C_{p,t}\right)}{\left(1 + \frac{k_{10}(\Delta t)}{2}\right)} \quad (2)$$

While most of the terms are known, the third bracket $\left(C_{p,t+1} - C_{p,t}\right)$, accounting for drug distribution into the peripheral compartment, needs to be solved before calculating $C_{c,t+1}$. In Loo-Riegelman original publication, the difference in C_p between two times was solved for t and t_{-1} (Loo and Riegelman, 1968). For the case of t_{+1} and t, the solution for $C_{p,t+1}$ can be written as:

$$C_{p,\,t+1} = \frac{k_{12}}{k_{21}} C_{c,t}\left(1 - e^{-k_{21}(\Delta t)}\right) + k_{12}\left(\frac{\left(C_{c,t+1} - C_{c,t}\right)(\Delta t)}{2}\right) + C_{p,\,t}\left(e^{-k_{21}(\Delta t)}\right) \quad (3)$$

Such that,

$$\left(C_{p,\,t+1} - C_{p,\,t}\right) = \frac{k_{12}}{k_{21}} C_{c,t}\left(1 - e^{-k_{21}(\Delta t)}\right) + k_{12}\left(\frac{\left(C_{c,t+1} - C_{c,t}\right)(\Delta t)}{2}\right) + C_{p,\,t}\left(e^{-k_{21}(\Delta t)} - 1\right) \quad (4)$$

Where k_{12} and k_{21} are distribution micro-constants as previously defined (Loo and Riegelman, 1968). Replacing Eq. (4) in Eq. (2) and rearranging gives the general expression to calculate $C_{c,t+1}$:

$$C_{c,t+1} = \frac{\Delta F_a\left(\frac{X_0}{V_c}\right) + C_{c,t}\left(1 - \frac{k_{10}(\Delta t)}{2} + \frac{k_{12}(\Delta t)}{2} - \frac{k_{12}}{k_{21}}\left(1 - e^{-k_{21}(\Delta t)}\right)\right) - C_{p,\,t}\left(e^{-k_{21}(\Delta t)} - 1\right)}{\left(1 + \frac{k_{10}(\Delta t)}{2} + \frac{k_{12}(\Delta t)}{2}\right)} \quad (5)$$

Solution of $C_{c,t+1}$ for the first plasma concentration point utilizes $t=t_{+1}$ and $t=0$, hence $C_{c,t}=0$, thus allowing calculation of the first $C_{c,t+1}$ value. Accordingly, this latter number becomes $C_{c,t}$ for calculation of the second plasma concentration point. Further details on derivation of Eq. (5) are given in the appendix (see Supplementary Materials).

2.1.2. Convolution equation from the exact Loo-Riegelman method

Eq. (6) shows the exact solution for Loo-Riegelman method in a two compartmental model published by J. Wagner (Wagner, 1983):

$$F_{a,t} = \frac{X_{a,t}}{X_{a,\infty}} = \frac{C_{c,t} + k_{10}\int_0^t C_c dt + k_{12}e^{-k_{21}t}\int_0^t C_c e^{k_{21}t} dt}{\left(k_{10}\int_0^\infty C_c dt\right)} \quad (6)$$

Likewise, the application of Gohel's reasoning on Eq. (6) and rearranging gives the following expression (see Supp. Materials for details):

$$\Delta F_a\left(\frac{X_0}{V_c}\right) = C_{c,t+1} - C_{c,t} + k_{10}\int_t^{t+1} C_c dt + k_{12}e^{-k_{21}t+1}\int_t^{t+1} C_c e^{k_{21}t} dt + k_{12}\left(e^{-k_{21}t+1} - e^{-k_{21}t}\right)\int_0^t C_c e^{k_{21}t} dt \quad (7)$$

Definite integrals between t and t_{+1} can be solved with linear trapezoid rule, resulting in the following general equation to calculate $C_{c,t+1}$. Accordingly, the Eq. (8) can be written for calculation of central compartment concentrations as function of fraction absorbed and time:

$$C_{c,t+1} = \frac{\Delta F_a\left(\frac{X_0}{V_c}\right) + C_{c,t}\left(1 - \frac{k_{10}(\Delta t)}{2} - \frac{k_{12}(\Delta t)}{2}\left(e^{k_{21}t}/e^{k_{21}t+1}\right)\right) - k_{12}\left(e^{-k_{21}t+1} - e^{-k_{21}t}\right)\int_0^t C_c e^{k_{21}t} dt}{\left(1 + \frac{k_{10}(\Delta t)}{2} + \frac{k_{12}(\Delta t)}{2}\right)} \quad (8)$$

2.2. Verification of equations

Eqs. (5) and (8) in this paper can be used for back-calculating plasma profiles from F_a vs time profiles for drugs with two-compartmental PK. Hence, verification was assessed by applying either original or exact Loo-Riegelman method on observed plasma data to deconvolute F_a vs time profiles for different cases (see below). Subsequently, plasma concentration profiles were reconstructed (convolution) using Eqs. (5) or (8). All digitalization and micro-constant fitting were carried out with Plot Digitizer V2.6.8 and Berkley Madonna V. 10.6.1, respectively. Further simulations and calculations were solved in Microsoft Excel®.

2.2.1. Immediate release dosage forms

Ketoprofen and amlodipine were used to exemplify cases with relatively rapid and slow distribution kinetics (Fig. S1). Plasma profiles after oral administration of ketoprofen 200 mg IR capsules (Houghton et al., 1984) and amlodipine 10 mg IR tablets were taken from the literature (Faulkner et al., 1986). Amlodipine intravenous administration profile was given in the same publication (Faulkner et al., 1986), hence it was used to fit amlodipine micro-constants k_{10}, k_{12} and k_{21} prior to deconvolution (Fig. S2). Conversely, given that ketoprofen intravenous data was reported somewhere else, micro-constants were taken from a different publication (Debruyne et al., 1987). While kinetic constants were obtained from the literature, we decided to calculate the V_c from our own $AUC_{0-\infty}$ in order to reduce the impact of population variability. Accordingly, V_c were calculated as $X_0/(AUC_{0-\infty}{*}k_{el})$, where k_{el} is the apparent elimination rate constant estimated from semi-logarithmic terminal slope.

2.2.2. Extended-release dosage forms

In addition, theophylline formulations with different release profiles (IR and extended-release, ER) were used to test the performance of Eqs. (5) and (8) (Hussein et al., 1987). Similarly, micro-constants were fit from intravenous infusion of theophylline (Mitenko et al., 1973) (Fig. S3) and V_c were calculated (see above). While trapezoidal values AUC values were consistent between IR and one ER formulation (Theotrim®, Israel), the other ER theophylline product (Theo-Dur®, U.S.) showed a trapezoidal AUC near 30% (even though same population was used). Therefore, both AUC and V_c values calculated for Theo-Dur® were assumed the same as those calculated for Theotrim®.

For each case, plasma profiles were recalculated using deconvoluted profiles and eqns derived in this manuscript. Resulting calculated plasma profiles were compared to observed profiles by two metrics: the root mean squared error (RMSE) and coefficient of determination (r^2).

2.3. Analysis of bioequivalence failure of immediate release contraceptive products using deconvolution/convolution

2.3.1. Materials

All reagents, including salts, buffers and HPLC grade solvents were purchased from Sigma-Aldrich, Merck KGaA (Darmstadt, Germany). Very same batches of the test and reference formulations were tested both in vitro and in vivo (see below). They were IR tablets containing a fixed dose combination of levonorgestrel 0.15 mg and ethinyl estradiol 0.03 mg. Both products were kindly provided by the sponsor under NDA.

2.3.2. In vitro dissolution

Among different in vitro conditions tested in this study, the most discriminative dissolution media was the inhouse-prepared simulated gastric fluid media containing HCl, pH 1.2, NaCl 60 mM and KCl 10 mM. Dissolution was studied in the USP type II apparatus (Teledyne Hanson's Super Precision Vessel™), using 900 ml of media at 37 °C and 50 rpm. In this study, the sample size was $n = 3$, based on the tight data dispersion (CV<12%) and the fact that this analysis does not aim to conduct any regulatory application. Samples were collected at 5, 15, 20, 30 and 90 min, filtered and analyzed with a Sciex Exion LC chromatographer coupled with a Sciex triple Quad 5500t mass spectrometer (Table S1).

2.3.3. Bioequivalence trial

Levonorgestrel PK profiles were obtained from a bioequivalence trial performed by the sponsor company. In short, test or reference tablets were administered to healthy volunteers ($n = 36$) in a single-dose, fasted-state, two-period, randomized, 2 × 2 cross-over designed bioequivalence trial. The study was performed according to ethical principles for medical research detailed in the World Medical Association declaration of Helsinki and approved by the Independent Ethics Committee (IEC), protocol HP8814–03, Version: 2 0.0, 04 December 2021. Blood samples were collected at 0.25, 0.5, 0.75, 1, 1.5, 2, 2.5, 3, 3.5, 4, 4.5, 5, 6, 8, 10, 12, 16, 24, 48, and 72 h, and plasma levonorgestrel concentrations were determined via HPLC-Ms/Ms. Observed PK parameters C_{max} and AUC_{0-t} were obtained by non-compartmental analysis and bioequivalence was evaluated as per regulatory guidelines (U.S. Department of Health and Human Services Food and Drug Administration Center for Drug Evaluation and Research (CDER), 2021). Products used in this study were contraceptive fixed dose (levonorgestrel/ethynyl estradiol). Because only levonorgestrel resulted in lack of bioequivalence, the deconvolution/convolution-based correlation approach was only applied on levonorgestrel data (see discussion for details on the case of ethynyl estradiol).

2.3.4. Deconvolution and convolution

Deconvolution/convolution approach proposed by Bermejo et al., (Bermejo et al., 2020b) for one-compartment PK drug, carbamazepine, was used to study bio-inequivalent levonorgestrel formulations. Briefly, plasma concentration versus time profiles were deconvoluted using

original Loo-Riegelman method. Due to the lack of intravenous (IV) data on these subjects, k_{10}, k_{12} and k_{21} micro-constant were fixed to literature values, 0.107, 0.434 and 0.178 h^{-1}, respectively (Liu et al., 2023).

In parallel, in vitro dissolution profiles were fit to a Weibull function (Langenbucher, 1972) to calculate in vitro times. These were used to scale-up in vitro times into equivalent in vivo times (Fig. S4). Then, resulting F_d vs scaled-time plots were fit to a second Weibull function to interpolate the equivalent fraction dissolved ($F_{d'}$). Values for all Weibull parameters are shown in Table S3. Subsequently correlated to deconvoluted F_a values in a linear model (Fig. S5). This procedure was previously detailed elsewhere (Bermejo et al., 2020b).

Finally, $F_{d'}$ values were converted into F_a by using the linear model. Volume of distribution (V_c) were calculated as previously sated (see above), to be 14.33 and 16.51 L for the reference and test product. Plasma levels of levonorgestrel were calculated for the reference and test products using Eq. (5). Prediction error (PE) for C_{max} and $AUC_{0\text{-}t}$ was assessed and compared to limits previously established (García et al., 2022; González-García et al., 2015; U.S. Department of Health and Human Services Food and Drug Administration Center for Drug Evaluation and Research (CDER), 1997).

3. Results

3.1. Original versus exact Loo-Riegelman deconvolution

Two scenarios were set in this manuscript to assess the performance of equations derived. Firstly, two drugs, ketoprofen and amlodipine, were chosen for representing cases of two-compartmental PK with relatively rapid and slow distribution rates, respectively (Fig. S1). Secondly, three theophylline formulations, including immediate and extended-release, were selected to cover diverse absorption rate profiles. Deconvoluted profiles with either original or exact Loo-Riegelman methods are shown in Fig. 1. Both methods produced very similar fraction absorbed-time profiles during the absorption phase, being them different only evident upon reaching the *plateau* phase. Point-by-point comparison of F_a at early stages of absorption is given in Table 1.

3.2. Verification of convolution Eq. (5) from original Loo-Riegelman

The Eq. (5) derived in this article was verified by back-calculating plasma concentrations after original Loo-Riegelman deconvolution. Fig. 2 shows that Eq. (5) accurately reconstructed plasma concentration profiles from F_a vs time profiles for both drugs, independent of their dissimilar distribution rates. In addition, the predictive potential was assessed for cases representing theophylline products with different release rates (Fig. 3A). As expected, the Eq. (5) was consistently able to reconstruct plasma profiles with a high degree of accuracy, regardless of differences in absorption rate profiles. In fact, calculations using Eq. (5) resulted in values for RMSE $<1.63 \times 10^{-16}$ and r^2 not lower than 1, respectively, for all cases studied. This demonstrates that approximations made to derive Eq. (5) resulted in a reliable back-calculation method for two-compartmental PK.

Table 1
Deconvoluted plasma profiles using either original or exact Loo-Riegelman methods.

Fraction ketoprofen absorbed			Fraction amlodipine absorbed		
Time (h)	Original LR	Exact LR	Time (h)	Original LR	Exact LR
0.25	0.0535	0.0535	0.5	0.0105	0.0105
0.5	0.4202	0.4203	1	0.0313	0.0313
0.75	0.6174	0.6178	2	0.0880	0.0881
1	0.7931	0.7938	4	0.2011	0.2017
1.5	0.8905	0.8938	5	0.2876	0.2883
2	0.9112	0.9152	6	0.3753	0.3760

LR: Loo-Riegelman.

3.3. Verification of convolution Eq. (8) from exact Loo-Riegelman

Furthermore, the Eq. (8) was derived from the exact solution for the Loo-Riegelman method. The equation was verified for the same cases aforementioned (Fig. 4). Similarly, the Eq. (8) allowed a precise convolution of plasma levels for all the cases studied. Statistical analysis showed that RMSE and r^2 values using Eq. (8) were $<7.71 \times 10^{-2}$ and >0.9996, respectively. Even though differences between observed and predicted became a bit higher compared to Eqn. (5), the Eqn. (8) was still able to reconstruct plasma levels in a extremely accurate fashion. A full comparison of observed and calculated PK parameters is given in Table 2 showing up to four decimal figures.

3.4. Application on deconvolution/convolution for levonorgestrel IR tablets

The second aim of this study was the application of methods here developed to predict plasma levels from in vitro dissolution profiles in a case of failed bioequivalence. Contraceptive fixed dose (levonorgestrel/ethynyl estradiol) reference and test products were tested in healthy humans. 30 out of 36 subjects completed the bioequivalence trial, where only levonorgestrel failed the bioequivalence criterion. Therefore,

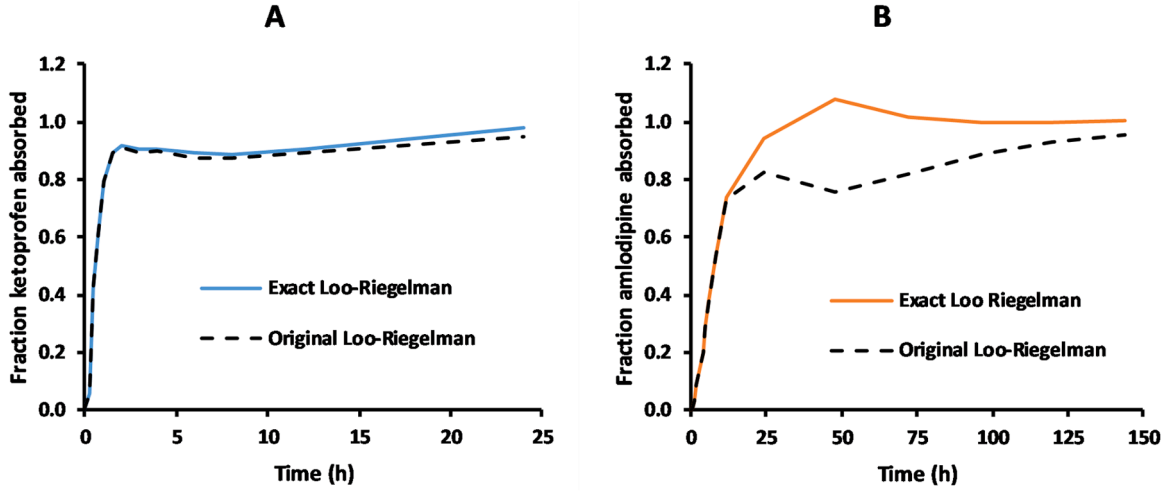

Fig. 1. Original (dashed lines) and exact Loo-Riegelman deconvolution (colored solid lines) for ketoprofen (A, blue) and amlodipine (B, orange) IR formulations orally administered (For interpretation of the references to color in this figure legend, the reader is referred to the web version of this article.).

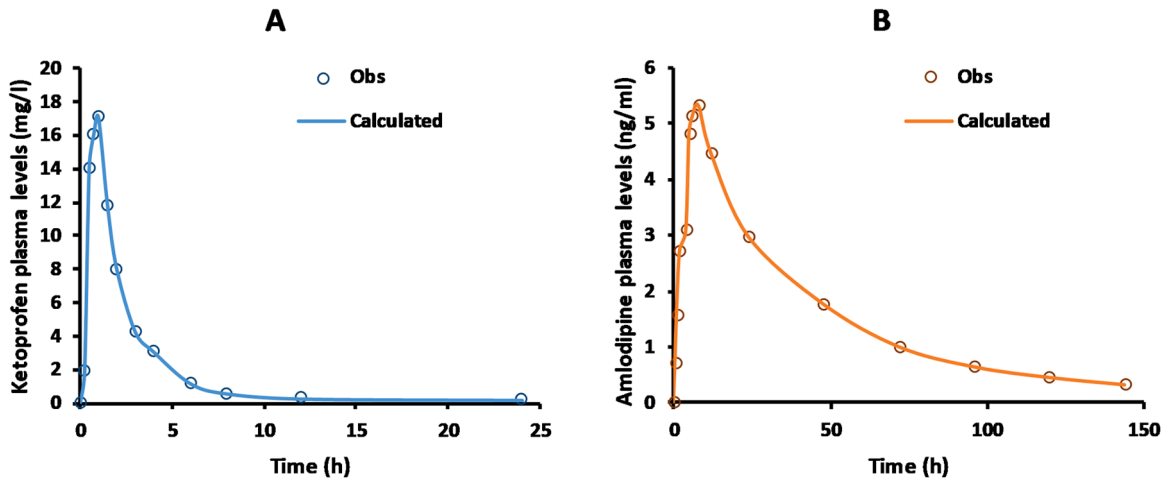

Fig. 2. Verification of Eq. (5) using ketoprofen (A, blue) and amlodipine (B, orange) IR formulations. Observed data (dots) was deconvoluted with original Loo-Riegelman and resulting F_a were directly input in Eq. (5) to reconstruct plasma profile (solid lines) (For interpretation of the references to color in this figure legend, the reader is referred to the web version of this article.).

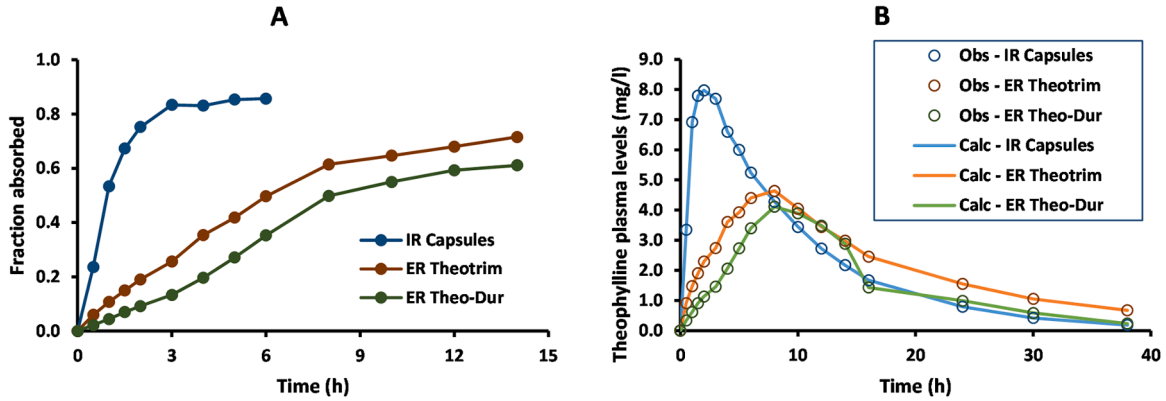

Fig. 3. Absorption and pharmacokinetics of theophylline formulations: IR capsules (blue), ER Theotrim® (red) and ER Theo-Dur® (green). Fraction absorbed were calculated using original Loo-Riegelman method (A). Calculated profiles (solid lines) were obtained with Eq. (5), predicting observed plasma profiles (dots) for different theophylline formulations (B) (For interpretation of the references to color in this figure legend, the reader is referred to the web version of this article.).

results presented in the main text only considered levonorgestrel, while outcomes with ethynyl estradiol were also included in supplementary material and discussed below.

Both observed levonorgestrel C_{max} and $AUC_{0\text{-}t}$ were higher for the reference compared to the test product (Table 3). This was consistent with in vitro dissolution of the test (orange) being slower than the reference (blue) from the 15 min mark, as seen in Fig. 5. Furthermore, Fig. 5 also depicts dissolution fit to Weibull distribution (Table S3), such that it can be used to calculate in vitro times (Fig. S4) and to construct a linear correlation model (Fig. S5). While the linear model was used to scale in vitro dissolution into in vivo absorption, Eq. (5) was used to handle the convolution into plasma levels. Fig. 6 shows how nicely this equation can be applied to predict plasma levels from in vitro dissolution profiles. Prediction errors with this approach can be seen in Table 3, where individual PE were all below 15% with absolute average PE below 10%(García et al., 2022; González-García et al., 2015; U.S. Department of Health and Human Services Food and Drug Administration Center for Drug Evaluation and Research (CDER), 1997).

4. Discussion

Convolution is a critical step in IVIVC, as its validation requires the reconstruction of plasma concentration-time profiles from in vitro profiles and the given correlation function. If successful, convolution step should allow the prediction of in vivo performance of different formulations tested in vitro under identical experimental conditions. Applications for convolution include, but are not limited to, predicting drug product performance, development and validation of IVIVC, rational drug development, safe space definition, SUPAC, among many other possibilities. Most typically, simulated plasma profiles are obtained with the convolution integral (Krishna and Yu, 2008). While that method can be solved numerically, it is not an analytical solution. Since analytical solutions can be presented as mathematical equations, they allow a clearer view of the interactions between variables and their effect on the outcome. Furthermore, they can be easily solved and algorithms for their computation are more efficient than numerical solutions. An analytical solution was previously developed for drugs with one-compartment PK (Gohel et al., 2005). This method has been used in several publications, including successful examples of IVIVC and prediction of plasma concentration profiles (González-García et al., 2015; Salehi et al., 2021; Sánchez-Dengra et al., 2021; Taha and Emara, 2022; Yaro et al., 2014), demonstrating its usefulness. However, that equation cannot be applied to most of drugs, as they commonly display two-compartmental PK (Liu et al., 2023). To the best of our knowledge, an equivalent solution for drugs with multiple compartment distribution has not been reported yet. In this work, we deduced simple, yet powerful, analytical solutions to apply compartmental convolution in two-, and even three- compartmental models (see below). Because of the

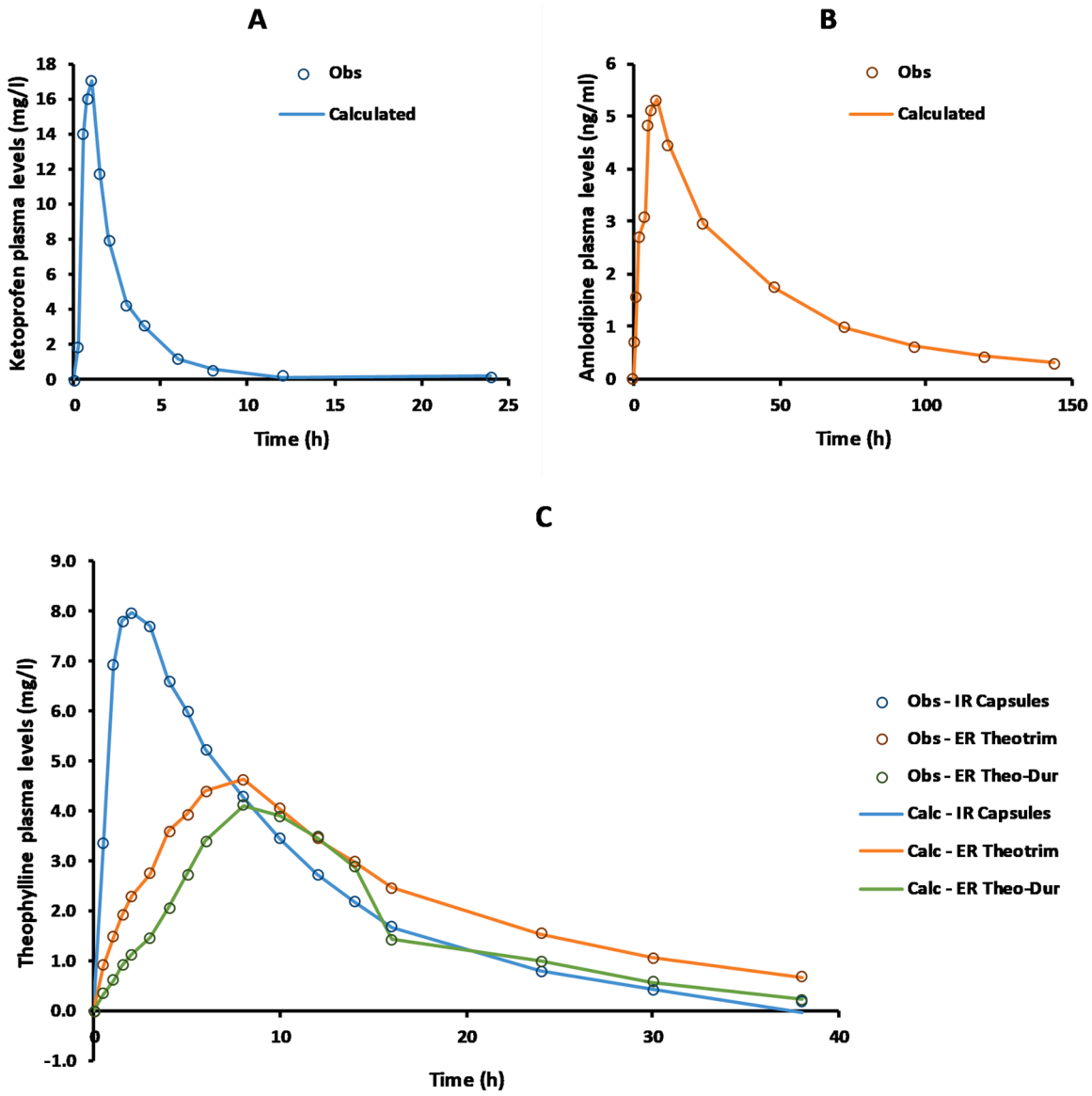

Fig. 4. Verification of Eq. (8) using ketoprofen (A) and amlodipine (B) IR formulations, as well as theophylline formulations with diverse absorption rates (C). Observed data (dots) was deconvoluted with the exact Loo-Riegelman and resulting F_a were directly input in Eq. (8) to reconstruct plasma profile (solid lines).

Table 2
Observed and calculated pharmacokinetic parameters after convolution using Eq. (5) or (8), respectively.

	C_{max}[a]			AUC_{0-t}[a]		
	Obs	Eq. (5)	Eq. (8)	Obs	Eq. (5)	Eq. (8)
KT	17.0497	17.0497	17.0497	42.699	42.699	42.699
AM[b]	5.3100	5.3100	5.3100	222.7475	222.7475	222.7475
T-IR	7.9757	7.9757	7.9757	85.9645	85.9645	85.0502
T-ER-1	4.6364	4.6364	4.6364	84.1411	84.1411	84.1411
T-ER-2	4.1105	4.1105	4.1105	60.9569	60.9569	60.9569

KT: Ketoprofen; AM: Amlodipine; T-IR: Theophylline immediate release; T-ER-1: Theophylline extended release Theotrim®; T-ER-2: Theophylline extended-release Theo-Dur®.

[a] : C_{max} and AUC_{0-t} have units of mg/l and mg*h/l, respectively, except for amlodipine ([b]).

[b] : C_{max} and AUC_{0-t} for these cases have units of ng/ml and ng*h/ml, respectively.

Table 3
Pharmacokinetic parameter for non-bioequivalent levonorgestrel IR products.

	C_{max} (ng/ml)			AUC_{0-t} (ng*h/ml)		
	Obs	Pred	PE (%)	Obs	Pred	PE (%)
Reference	6.61	6.61	0.01	100.2	110.6	10.4
Test	5.35	4.62	-13.6	87.62	86.32	-1.48
Absolute average	-	-	-6.80	-	-	4.46
Ratio T/R	0.80	0.70	-	0.87	0.78	-

advantages related to having analytical solutions for this procedure, it is expected that equations provided in this manuscript are going to be very useful for pharmaceutical scientists.

4.1. *Verification of convolution approaches: Eqs. (5) and (8)*

The starting point of this work were both original (Loo and Riegelman, 1968) and exact solutions (Wagner, 1983) to Loo-Riegelman deconvolution. Fig. 1 and Table 1 showed that deconvolution approaches for the absorption phase are not exactly equal but greatly

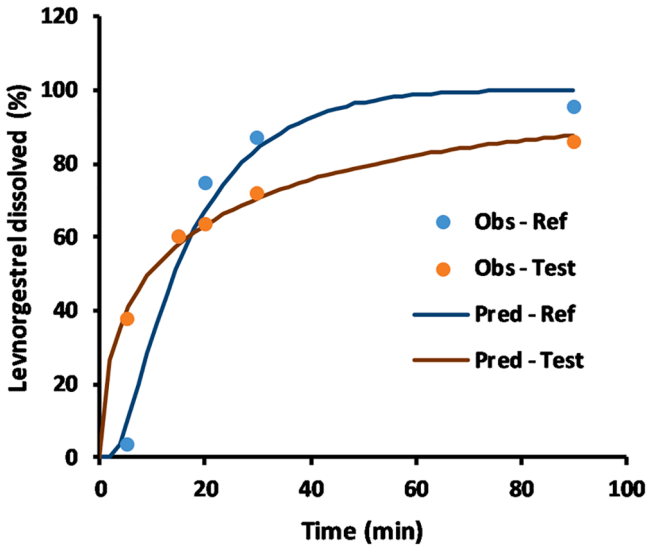

Fig. 5. Average levonorgestrel dissolution from reference (blue) and test tablets (orange) in simulated gastric media ($n = 3$) and their respective fitting to Weibull model (solid lines) (For interpretation of the references to color in this figure legend, the reader is referred to the web version of this article.).

comparable. However, profiles tended to diverge upon reaching the *plateau*, most likely due to the linear versus exponential contribution of the time in original and exact methods, respectively. In Wagner's publication (Wagner, 1983), integrals in the exact Loo-Riegelman solution are solved by using combination of linear and logarithmic trapezoid rules (lin-up, log-down). By contrast, we decided to use only the linear trapezoid rule because, otherwise, derivation of convolution equation will take the form of $\ln(x) - ax = b$, which solution requires the multi-valued Lambert W function. Nonetheless, linear approximation in deconvolution does not explain the divergence at the *plateau* between the exact and original deconvolution methods (data not shown).

Another aim of this study was to verify equations here developed across different cases. When re-distribution is much faster than elimination, plasma concentrations can be easily described by one-compartmental models. However, as distribution becomes comparable to elimination, two or even three compartments might be needed to better describe plasma profiles. In this manuscript, ketoprofen and amlodipine served as model drugs for two-compartment PK, having them relatively rapid and slow redistribution, respectively (Liu et al., 2023; Mitenko et al., 1973). While ketoprofen exhibits a fraction absorbed of 92% (Shohin et al., 2012), amlodipine's is only around 62.5% (mainly due to first pass extraction, since 96% of drug is absorbed) (Beresford et al., 1988). Moreover, distribution into peripheral compartment is much more favored for amlodipine than ketoprofen, with k_{12}/k_{21} ratios being 15 and 1, respectively. Irrespective of the case, both Eqs. (5) and (8) accurately predicted plasma concentrations curves (Figs. 2 and 4). This demonstrates that analytical solutions here proposed are correctly developed and can be used to convolute fraction absorbed data into predicted plasma profiles. To further explore the scope of our solutions, theophylline plasma profiles after administration of IR capsules or ER formulations were analyzed too. Similar to ketoprofen, theophylline has an oral bioavailability of 96% (Hendeles L et al., 1977). However, calculation of $AUC_{0\text{-}t}$ for theophylline products were 86.9, 87.5, and 62.1 mg*h/l, for the IR capsule, ER Theotrim® and ER Theo-Dur® formulations, respectively. This is because of the much slower release of the latter product, *ergo* incomplete absorption (Fig. 3). For cases like this, the application of Loo-Riegelman deconvolution

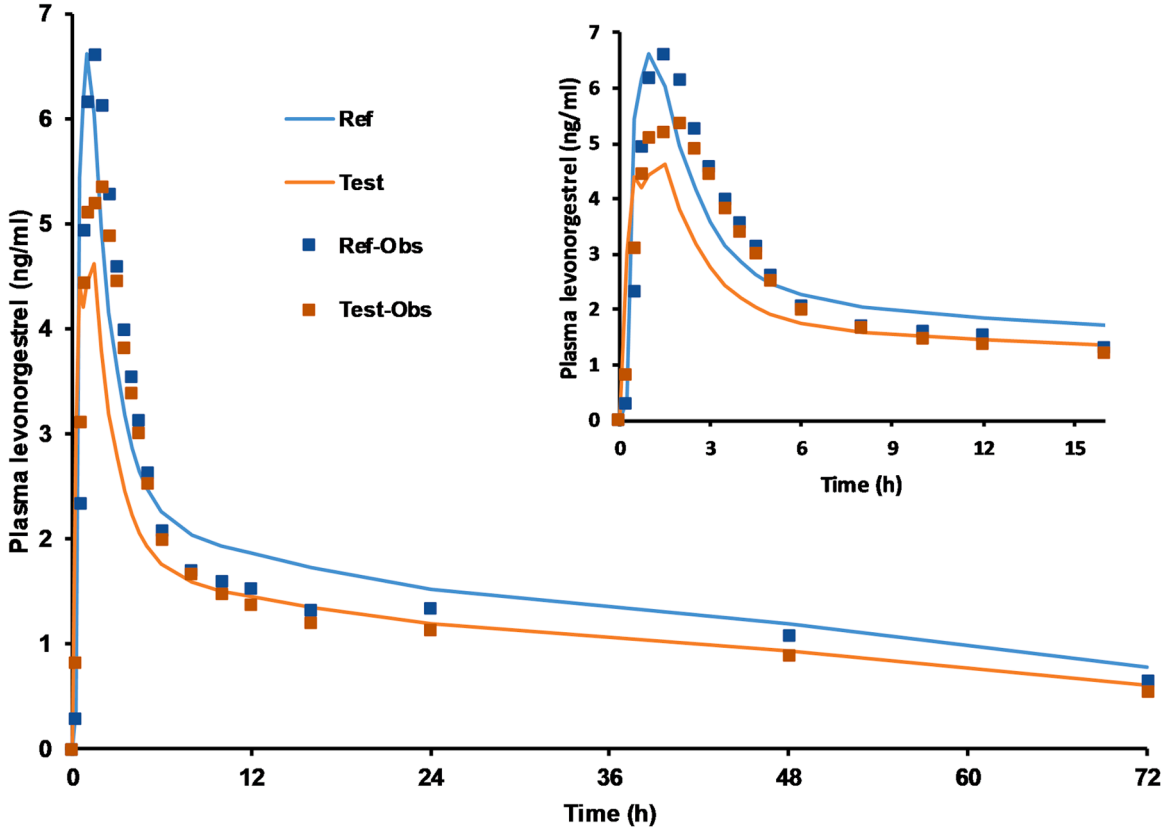

Fig. 6. Plasma concentration versus time profiles for levonorgestrel from the reference (blue) and test products (orange). Solid lines represent profiles calculated with Eq. (5), while squares show average observed data ($n = 30$). Figure insert shows a zoom-in to allow better visualization of early timepoints (For interpretation of the references to color in this figure legend, the reader is referred to the web version of this article.).

overestimates the absorption rate. Hence, the $AUC_{0\text{-inf}}$ was assumed to be equal to the other ER product, in order to have a better estimation of the absorption rate (Fig. 3A). Given that the volume of central compartment was also calculated from the $AUC_{0\text{-inf}}$ (see methods), this assumption changed the value of V_c too. Nonetheless, the equation was able to reconstruct plasma profiles regardless of the absorption rate, as long as the V_c value used in Eqs. (5) or (8) remained consistent with the V_c used in the deconvolution (Figs 3 and 4C). Alternatively, V_c may also be obtained by fitting to two-compartmental model, which leads to V_c values ($V_{c,fit}$) different from those calculated in this manuscript. While V_c calculation method employed in this work was chosen for it to reduce the impact of population variability, $V_{c,fit}$ values are still suitable to be used in our convolution eqns. However, this modification must be considered in the Loo-Riegelman deconvolution, as well, for the convolution to work. For this purpose, the trapezoidal $AUC_{0\text{-}\infty}$*k_{10} term in deconvolution should be replaced by ($X_0/V_{c,fit}$) to account for the total mass absorbed into the central compartment with a volume $V_{c,fit}$. This correction maintains the consistency of V_c, such that plasma profiles can be accurately reconstructed (data not shown). Therefore, both equations derived in this paper can be successfully applied to different cases of two compartmental drugs as long as the Loo-Riegelman's deconvolution remains valid and input parameters remain consistent with it.

In this article, two analytical solutions are proposed for convolution based on either the original or exact Loo-Riegelman deconvolution. While Eq. (5) from original Loo-Riegelman gives slightly better predictions than Eq. (8), it is clear that both are extremely accurate for convoluting plasma profiles that were deconvoluted with each respective method (Figs. 1–4 and Table 2). Given that the exact Loo-Riegelman deconvolution advantages the original method (Wagner, 1983), Eq. (8) should be preferred over Eq. (5). It is worthwhile to note that convolution via Eq. (5) requires information on apparent peripheral concentrations (C_p). Although Eq. (4) can be used to calculate the value of C_p over time, the physical interpretation of that parameter is not as straightforward as it seems. In fact, C_p cannot be interpreted as real peripheral concentrations because it is defined as the mass that reaches the second compartment over the volume of the central compartment. Therefore, this parameter actually represents the concentration of drug that leaves the central compartment. By contrast, Eq. (8) lacks this term and, hence, an equation for calculating drug in peripheral compartment is not needed. This result in an advantage for the exact solution, Eq. (8), where the physical meaning of parameters is easier to be interpreted. Furthermore, Eq. (8) provides a smoother handling of mathematical terms, leading to an easier generalization. For instance, the same approach can be used to deduce an expression for three-compartmental model, as depicted in Eq. (9):

$$C_{c,t+1} = \frac{\Delta F_a\left(\frac{X_0}{V_c}\right) + C_{c,t}\left(1 - \frac{k_{10}(\Delta t)}{2} - \frac{k_{12}(\Delta t)}{2}\left(e^{k_{21}t}/e^{k_{21}t+1}\right) - \frac{k_{13}(\Delta t)}{2}\left(e^{k_{31}t}/e^{k_{31}t+1}\right)\right) - k_{12}\left(e^{-k_{21}t+1} - e^{-k_{21}t}\right)\int_0^t C_c e^{k_{21}t}dt - k_{13}\left(e^{-k_{31}t+1} - e^{-k_{31}t}\right)\int_0^t C_c e^{k_{31}t}dt}{\left(1 + \frac{k_{10}(\Delta t)}{2} + \frac{k_{12}(\Delta t)}{2} + \frac{k_{13}(\Delta t)}{2}\right)} \quad (9)$$

Accordingly, it is clear that Eq. (9) is an extension of Eq. (8), where the terms $-\frac{k_{13}(\Delta t)}{2}\left(e^{k_{31}t}/e^{k_{31}t+1}\right)$, $-k_{13}\left(e^{-k_{31}t+1} - e^{-k_{31}t}\right)\int_0^t C_c e^{k_{31}t}dt$, and $\frac{k_{13}(\Delta t)}{2}$ were introduced. This suggests this eqn can be easily generalizable to n^{th} compartment for a drug with k_{1n} and k_{n1} distribution micro-constants by simply adding the respective terms accounting for the n compartments. On the other hand, Eq. (5) can also be expanded for three-compartment PKs, as shown below in Eq. (10):

$$C_{c,t+1} = \frac{\Delta F_a\left(\frac{X_0}{V_c}\right) + C_{c,t}\left(1 - \frac{k_{10}(\Delta t)}{2} + \frac{k_{12}(\Delta t)}{2} + \frac{k_{13}(\Delta t)}{2} - \frac{k_{12}}{k_{21}}\left(1 - e^{-k_{21}(\Delta t)}\right) - \frac{k_{13}}{k_{31}}\left(1 - e^{-k_{31}(\Delta t)}\right)\right) - C_{p2,\,t}\left(e^{-k_{21}(\Delta t)} - 1\right) - C_{p3,\,t}\left(e^{-k_{31}(\Delta t)} - 1\right)}{\left(1 + \frac{k_{10}(\Delta t)}{2} + \frac{k_{12}(\Delta t)}{2} + \frac{k_{13}(\Delta t)}{2}\right)} \quad (10)$$

Where C_{p2} and C_{p3} are drug concentrations leaving to compartment 2 and 3, respectively. Therefore, even though an extension of Eq. (5) is also fairly straightforward to be deduced, calculation of drug in central compartment will require to know drug concentration leaving to each compartment, which in turn makes calculations less efficient.

4.1.1. Novel aspects and potential impact

Equations derived in this manuscript offer a more correct approach to performing convolution of release/absorption profiles when a two or three-compartment deconvolution was already applied. Either original or exact Loo-Riegelman methods are typically used to deconvolute plasma curves, thus allowing correlation to in vitro dissolution profiles. However, convolution is commonly handled by the non-compartmental convolution integral, which is not analytical, but numerically solved. Therefore, this work comes to fill this gap by providing analytical solutions based on the inverse of both the original and exact Loo-Riegelman methods. Analytical solutions are simple and straightforward allowing the scientist to perform (and the regulator to understand) a convolution without having strong modelling skills or training in specialized modelling software. In addition, their clarity and lack of dependence on algorithms makes them more tamper-proof and provides for enhanced transparency both in regulatory submissions and in scholarly research articles. In this work, micro-constants were obtained by curve fitting to ordinary differential equations (ODE). Nevertheless, they may be estimated from α and β macro-constants, thus avoiding the need of using fitting software. In the same line, it is a common practice to apply model fitting to dissolution/absorption curves when applying an ODE-based convolution. Equations described in this paper lead to a less model-dependent approach, that can even obviate the need of any fitting provided a sufficient number of timepoints. Furthermore, our methods are independent from the first order assumption for absorption, represented by k_a, because they are based on the mass balance approach previously proposed (Gohel et al., 2005; Loo and Riegelman, 1968; Wagner, 1983; Wagner and Nelson, 1963). This first order assumption has been recently questioned by some authors who argued that absorption should occur in a finite time with zero-order kinetics (Chryssafidis et al., 2022; Macheras and Chryssafidis, 2020). The eqns

we developed in this manuscript do not exclude that possibility as they do not assume any particular absorption kinetic model.

4.2. Application of convolution to non-bioequivalent levonorgestrel IR tablets

One of the examples of using mono-compartmental convolution was the study published by Bermejo et al., where an IVIVC was developed for non-bioequivalent carbamazepine IR tablets (Bermejo et al., 2020b). In their publication, they were able to correlate in vitro dissolution and in vivo fraction absorbed by applying a two-step method with linear time-scaling using Levy's plot. In the present work, we applied a similar approach for the two-compartmentally distributed drug, levonorgestrel (Liu et al., 2023). Two compartmental distribution of this drug was clearly observed in Fig. S6, as two different decay rates can be identified before and after 12 hours, approximately. Given that both solutions in this manuscript showed comparable performance (see above), the original method, Eq. (5), was used for this application. It is well-known that in vitro dissolution times are often different from in vivo times, with the former being usually shorter than the latter. Unlike direct convolution methods, where time-scaling can be included as part of the convolution integral or in curve fitting functions (Al-Gousous and Langguth, 2018; Cámara-Martinez et al., 2022; Sánchez-Dengra et al., 2021), successful prediction of plasma-time profiles demands that in vitro dissolution and in vivo absorption take place at comparable time-scales. That is why, the Levy's relation was included in our approach (Fig. S4), likewise it was incorporated in Bermejo's paper (Bermejo et al., 2020b). As seen in Fig. 6, the application of Eq. (5) on in vitro dissolution/absorption profiles resulted in remarkable predictions of plasma curves. In fact, individual PE were below 15% with absolute average PE values below 10% (Table 3) (González-García et al., 2015). The C_{max} PE displayed the largest error in this study, with a simulated value underpredicting the observed C_{max} by 13.6%. This minor deviation is caused by the slow dissolution between 20 and 90 min, as the percentage dissolved kept increasing from 64 to 88% during that time interval. When coupled with a two-compartmental disposition model, the amount slowly absorbed within that timeframe is distributed into the second compartment and/or eliminated, leading to a simulated C_{max} lower than the observed. The second largest PE was the $AUC_{0\text{-}t}$ for the reference product, where simulated value was 10.4% higher than the observed. In this case, the slight deviation may be explained by the fact that distribution coefficients k_{12} and k_{21} were taken unmodified from literature (Liu et al., 2023), and do not necessarily reflect distribution coefficients in the population where the bioequivalence trial was conducted. In fact, Fig. 6 clearly shows that overprediction occurred between the 6th and 24th hour. This behavior was not seen with the test formulation, because it was prevented by the slower dissolution/absorption. In spite of these non-significant deviations, all individual and absolute average PE fell within the limits typically accepted.

The same analysis performed on levonorgestrel non-bioequivalent profiles was further applied to bioequivalent ethynyl estradiol profiles (Supp. Material). As anticipated, it was not possible to establish a correlation between in vitro and in vivo profiles, because absorption was not limited by dissolution (Fig. S7). Actually, if the correlation were to be applied anyways to convolute plasma profiles with our method, simulated C_{max} resulted in large overpredictions for both reference and test formulations, with PE 102 and 78%, respectively. Nonetheless, test/reference ratios on simulated PK parameters were consistent with ethynyl estradiol bioequivalence (Table S4 and Fig. S8). This observation demonstrates that interpretation of PE values should be constrained to validating the correlation and do not necessarily resemble the bioequivalence outcome. In fact, ratio test/reference ratios for levonorgestrel were also in line with the lack of bioequivalence (Table 3), though C_{max} PE values were much lower than those obtained with ethynyl estradiol (Table S4).

4.2.1. Chemistry, manufacturing and control aspects

Last but not least, the cause of bio-inequivalence in the clinical trial was not clear, although the effect of excipients and/or particle size cannot be ruled out. For instance, the test product used sodium croscarmellose as super-disintegrant. This may explain the early boost in dissolution at 5 min (F_d=38%), while larger particles would explain the slow levonorgestrel dissolution between 15 and 90 min (Fig. 5). Other mechanisms involving croscarmellose cannot be discarded, as well. For instance, levonorgestrel does not have any relevant ionizable group at physiologically relevant pH values, however only hydrochloric acid media, and not phosphate or acetate, was able to correctly rank product dissolution (data not shown). One possible explanation for biopredictivity of this media are relatively high concentrations of croscarmellose in test product. In acidic media, unionized form of croscarmellose is predominant, resulting in lower polymer swelling (compared to higher pH media) and, thus exerting weaker tablet-disrupting action, as it was previously shown for hydrochlorothiazide tablets (Zhao and Augsburger, 2005). Also importantly, media ionic strength (IS) was adjusted to simulate gastric luminal contents. This might also play a role on media biorelevance, since it has been suggested that the higher the IS, the lower the super-disintegrant swelling capacity (Berardi et al., 2021). Further research on these hypotheses may clarify whether one of these mechanisms underlies the bio-inequivalence seen between levonorgestrel products and/or whether that potential interaction can be generalized to other BCS class II drug products formulated with ionizable super-disintegrants.

5. Conclusions

This manuscript shows the derivation of novel analytical solutions for compartmental convolution of plasma concentrations from original and exact Loo-Riegelman methods. Both equations were extremely accurate in reconstructing plasma profiles after their corresponding deconvolution method. However, the exact Loo-Riegelman method, here Eq. (8), is slightly advantaged because of its easier interpretability and mathematical manipulation to extend the model to several compartments. In fact, equations for three-compartments, Eq. (9) and (10), were also deduced in this paper. Nonetheless, Eq. (5) derived from original method did also work fine, as it was demonstrated by its successful application in the convolution of levonorgestrel plasma profiles from non-bioequivalent formulations. These analytical convolution methods that allow comprehensive understanding of the effect of variables and their interaction on final outcomes may be highly appreciated by pharmaceutical scientists.

CRediT authorship contribution statement

Mauricio A. García: Writing – original draft, Visualization, Validation, Supervision, Software, Resources, Project administration, Methodology, Investigation, Funding acquisition, Formal analysis, Data curation, Conceptualization. **Pablo M. González:** Writing – review & editing, Resources, Formal analysis, Data curation. **Alexis Aceituno:** Writing – review & editing, Validation. **Jozef Al-Gousous:** Writing – review & editing, Methodology, Investigation.

Declaration of competing interest

The authors declare no conflicts of interest.

Data availability

Some data can be shared upon request. Some other is confidential.

Acknowledgments

This research was funded by "Agencia Nacional de Investigación y Desarrollo" (ANID), Chile, Fondecyt Iniciación Project n° 11240418 and "Pontificia Universidad Católica de Chile", "Proyecto de Inserción Académica (PIA)" n° 3915-1004-301-81. Authors thank Dr. James Polli for the insightful discussions and Ms. Danae Contreras, PharmD, for her support on data organization.

Supplementary materials

Supplementary material associated with this article can be found, in the online version, at doi:10.1016/j.ejps.2024.106892.

References

Al-Gousous, J., Langguth, P., 2018. A time-scaled convolution approach to construct IVIVC for enteric-coated acetylsalicylic acid tablets. Pharmazie 73, 67–69. https://doi.org/10.1691/ph.2018.7136.

Berardi, A., Bisharat, L., Quodbach, J., Abdel Rahim, S., Perinelli, D.R., Cespi, M., 2021. Advancing the understanding of the tablet disintegration phenomenon – an update on recent studies. Int. J. Pharm. https://doi.org/10.1016/j.ijpharm.2021.120390.

Beresford, A.P., McGibney, D., Humphrey, M.J., Macrae, P., Stopher, D.A., 1988. Metabolism and kinetics of amlodipine in man. Xenobiotica 18, 245–254.

Bermejo, M., Hens, B., Dickens, J., Mudie, D., Paixão, P., Tsume, Y., Shedden, K., Amidon, G.L., 2020a. A mechanistic physiologically-based biopharmaceutics modeling (PBBM) approach to assess the in vivo performance of an orally administered drug product: from IVIVC to IVIVP. Pharmaceutics 12. https://doi.org/10.3390/pharmaceutics12010074.

Bermejo, M., Meulman, J., Davanço, M.G., Carvalho, P., de, O., Gonzalez-Alvarez, I., Campos, D.R., 2020b. In vivo predictive dissolution (Ipd) for carbamazepine formulations: additional evidence regarding a biopredictive dissolution medium. Pharmaceutics 12, 1–21. https://doi.org/10.3390/pharmaceutics12060558.

Cámara-Martinez, I., Blechar, J.A., Ruiz-Picazo, A., Garcia-Arieta, A., Calandria, C., Merino-Sanjuan, V., Langguth, P., Gonzalez-Alvarez, M., Bermejo, M., Al-Gousous, J., Gonzalez-Alvarez, I., 2022. Level A IVIVC for immediate release tablets confirms in vivo predictive dissolution testing for ibuprofen. Int. J. Pharm. 614 https://doi.org/10.1016/j.ijpharm.2021.121415.

Chryssafidis, P., Tsekouras, A.A., Macheras, P., 2022. Re-writing oral pharmacokinetics using physiologically based finite time pharmacokinetic (PBFTPK) models. Pharm. Res. 39, 691–701. https://doi.org/10.1007/s11095-022-03230-0.

Davanço, M.G., Campos, D.R., Carvalho, P.O., 2020. In vitro – in vivo correlation in the development of oral drug formulation: A screenshot of the last two decades. Int. J. Pharm. 580, 119210 https://doi.org/10.1016/j.ijpharm.2020.119210.

Debruyne, D., de Ligny, B.H., Ryckelynck, J.P., Albessard, F., Moulin, M., 1987. Clinical pharmacokinetics of ketoprofen after single intravenous administration as a bolus or infusion. Clin. Pharmacokinet. 12, 214–221. https://doi.org/10.2165/00003088-198712030-00003.

Faulkner, J., McGibney, D., Chasseaud, L., Perry, J., Taylor, I., 1986. The pharmacokinetics of amlodipine in healthy volunteers after single intravenous and oral doses and after 14 repeated oral doses given once daily. Br. J. Clin. Pharmacol. 22, 21–25. https://doi.org/10.1111/j.1365-2125.1986.tb02874.x.

García, M.A., Bolger, M.B., Suarez-Sharp, S., Langguth, P., 2022. Predicting pharmacokinetics of multisource acyclovir oral products through physiologically based biopharmaceutics modeling. J. Pharm. Sci. 111, 262–273. https://doi.org/10.1016/j.xphs.2021.10.013.

Gohel, M., Delvadia, R., Parikh, D., Zinzuwadia, M., Soni, C., Sarvaiya, K., Mehta, N., Joshi, B., Dabhi, A., 2005. Back Calculations in Wagner-Nelson Method : Applications in IVIVC.

González-García, I., Mangas-Sanjuán, V., Merino-Sanjuán, M., Bermejo, M., 2015. In vitro-in vivo correlations: General concepts, methodologies and regulatory applications. Drug Dev. Ind. Pharm. https://doi.org/10.3109/03639045.2015.1054833.

Hendeles, L, Weinberger, M., Bighley, L., 1977. Absolute bioavailability of oral theophylline. Am. J. Hosp. Pharm. 34, 525–527.

Houghton, G.W., Dennis, M.J., Rigler, E.D., Parsons, R.L., 1984. Comparative pharmacokinetics of ketoprofen derived from single oral doses of ketoprofen capsules or a novel sustained-release pellet formulation. Biopharm. Drug Dispos. 5, 203–209. https://doi.org/10.1002/bdd.2510050302.

Hussein, Z., Bialer, M., Friedman, M., Raz, I., 1987. Comparative pharmacokinetic evaluation of sustained-release theophylline formulations in dogs and humans. Int. J. Pharm. 37, 97–102. https://doi.org/10.1016/0378-5173(87)90013-5.

Krishna, R., Yu, L., 2008. Biopharmaceutics Applications in Drug Development. Springer, US, Nwe York, NY.

Langenbucher, F., 2003. Handling of computational in vitro/in vivo correlation problems by Microsoft Excel: III. Convolution and deconvolution. Eur. J. Pharmaceut. Biopharmaceut. 56, 429–437. https://doi.org/10.1016/S0939-6411(03)00140-1.

Langenbucher, F., 1972. Linearization of dissolution rate curves by the Weibull distribution. J. Pharm. Pharmacol. 24, 979–981.

Liu, F., Yi, H., Wang, L., Cheng, Z., Zhang, G., 2023. A novel method to estimate the absorption rate constant for two-compartment model fitted drugs without intravenous pharmacokinetic data. Front. Pharmacol. 14 https://doi.org/10.3389/fphar.2023.1087913.

Loo, J.C.K., Riegelman, S., 1968. New method for calculating the intrinsic absorption rate of drugs. J. Pharm. Sci. 57, 918–928.

Macheras, P., Chryssafidis, P., 2020. Revising pharmacokinetics of oral drug absorption: I models based on biopharmaceutical/physiological and finite absorption time concepts. Pharm. Res. 37, 187. https://doi.org/10.1007/s11095-020-02894-w/Published.

Madny, M.A., Deshpande, P., Tumuluri, V., Borde, P., Sangana, R., 2022. Physiologically based biopharmaceutics model of vildagliptin modified release (MR) tablets to predict in vivo performance and establish clinically relevant dissolution specifications. AAPS. PharmSciTech. 23 https://doi.org/10.1208/s12249-022-02264-2.

Mitenko, P.A., Ogilvie, R.I., Montreal, C., 1973. Pharmacokinetics of intravenous theophylline. Clin. Pharmacol. Ther. 14, 509–513.

Qureshi, S.A., 2010. In vitro-in vivo correlation (IVIVC) and determining drug concentrations in blood from dissolution testing-A simple and practical approach. Open Drug Deliv. J.

Salehi, N., Kuminek, G., Al-Gousous, J., Sperry, D.C., Greenwood, D.E., Waltz, N.M., Amidon, G.L., Ziff, R.M., Amidon, G.E., 2021. Improving dissolution behavior and oral absorption of drugs with pH-dependent solubility using pH modifiers: a physiologically realistic mass transport analysis. Mol. Pharm. 18, 3326–3341. https://doi.org/10.1021/acs.molpharmaceut.1c00262.

Sánchez-Dengra, B., González-García, I., González-Álvarez, M., González-Álvarez, I., Bermejo, M., 2021. Two-step in vitro-in vivo correlations: Deconvolution and convolution methods, which one gives the best predictability? Comparison with one-step approach. Eur. J. Pharmaceut. Biopharmaceut. 158, 185–197. https://doi.org/10.1016/j.ejpb.2020.11.009.

Shohin, I.E., Kulinich, J.I., Ramenskaya, G.V., Abrahamsson, B., Kopp, S., Langguth, P., Polli, J.E., Shah, V.P., Groot, D.W., Barends, D.M., Dressman, J.B., 2012. Biowaiver monographs for immediate-release solid oral dosage forms: ketoprofen. J. Pharm. Sci. 101, 3593–3603.

Sjögren, E., Abrahamsson, B., Augustijns, P., Becker, D., Bolger, M.B., Brewster, M., Brouwers, J., Flanagan, T., Harwood, M., Heinen, C., Holm, R., Juretschke, H., Kubbinga, M., Lindahl, A., Lukacova, V., Münster, U., Neuhoff, S., Anh, M., Peer, A. Van, Reppas, C., Rostami, A., Tannergren, C., Weitschies, W., Wilson, C., Zane, P., Lennernäs, H., Langguth, P., 2014. In vivo methods for drug absorption – Comparative physiologies, model selection, correlations with in vitro methods (IVIVC), and applications for formulation/API/excipient characterization including food effects. Eur. J. Pharmaceut. Sci. 57, 99–151. https://doi.org/10.1016/j.ejps.2014.02.010.

Taha, N.F., Emara, L.H., 2022. Convolution- and deconvolution-based approaches for prediction of pharmacokinetic parameters of Diltiazem extended-release products in flow-through cell dissolution tester. AAPS. PharmSciTech. 23 https://doi.org/10.1208/s12249-022-02361-2.

U.S. Department of Health and Human Services Food and Drug Administration Center for Drug Evaluation and Research (CDER), 2021. Bioequivalence Studies With Pharmacokinetic Endpoints for Drugs Submitted Under an ANDA. Guidance for Industry - DRAFT GUIDANCE.

U.S. Department of Health and Human Services Food and Drug Administration Center for Drug Evaluation and Research (CDER), 1997. Guidance for Industry - Extended Release Oral Dosage Forms: Development, Evaluation, and Application of In Vitro/In Vivo Correlations. Tel.

U.S. Department of Health and Human Services Food and Drug Administration Center for Drug Evaluation and Research (CDER), 1995. Guidance for industry - immediate release solid oral dosage forms. scale-up and postapproval changes: chemistry, manufacturing, and controls. Vitro Dissolution Testing, and In Vivo Bioequivalence Documentation.

Wagner, J.G., 1983. Pharmacokinetic absorption plots from oral data alone or oral/intravenous data and an exact Loo-Riegelman equation. J. Pharm. Sci. 72, 836.

Wagner, J.G., Nelson, E., 1963. Per cent absorbed time plots derived from blood level and/or urinary excretion data. J. Pharm. Sci. 52, 610–611. https://doi.org/10.1002/jps.2600520629.

Yaro, P., He, X., Liu, W., Xun, M., Ma, Y., Li, Z., Shi, X., 2014. In vitro-in vivo correlations for three different commercial immediate-release indapamide tablets. Drug Dev. Ind. Pharm. 40, 1670–1676. https://doi.org/10.3109/03639045.2013.842577.

Zhao, N., Augsburger, L.L., 2005. The. Influence of Swelling Capacity of Superdisintegrants in Different pH Media on the Dissolution of Hydrochlorothiazide From Directly Compressed Tablets.